

SURFACE-INTERFACE MICROSTRUCTURES AND FRICTION-WEAR PERFORMANCES OF THERMAL SPRAYED FECRBSI COATINGS OBTAINED BY HIGH-VELOCITY OXYGEN FUEL PROCESS

Liu Wenming,¹ Sheng Tianyuan,¹ and Kong Dejun^{2,3}

UDC 621.793.72:5333.9;620.178.1

A layer of FeCrBSi coating was prepared on H13 hot work steel using a high-velocity oxygen fuel spraying (HVOF). The morphologies and distribution of chemical elements and phases in the obtained coatings were analyzed using a field emission scanning electron microscopy (FMSEM), energy dispersive spectrometry (EDS), and X-ray diffraction (XRD), respectively. The friction-wear performance of FeCrBSi coating was examined using a wear test, and the wear mechanism was also discussed. The results show that the coating is primarily composed of Fe, Cr, B, and Si elements, which are uniformly distributed in the coating, enriched in the coating, and poor in the substrate at the coating interface. Among them, the Fe content decreases gradually in the substrate-coating direction, the Fe content of the coating is 40% lower than that of the substrate. The Cr, B, and Si contents in the coating are higher than those in the substrate, which form compounds and diffusion at the interface; as a result, the coating is combined with the substrate in the form of metallurgical bonding. The coating has a good friction reduction and wear resistance, the average COF (coefficient of friction) is 0.2126, the wear rate is $1.5 \cdot 10^{-6} \text{ mm}^3/\text{sec} \cdot \text{N}$, and the wear mechanism consists abrasive wear and spalling.

Keywords: high-velocity oxygen fuel (HVOF), FeCrBSi coating, surface-interface morphology, friction and wear.

INTRODUCTION

The H13 hot work die steel with high strength and ductility is primarily composed of Cr, Mo, Si, and V alloy elements, and is widely used for hot forging mould, hot extrusion mould, nonferrous metal casting mould, etc. However, the mold often fails due to wear during the metal forming; hence, how to improve its wear resistance and prolong service life has become an important research hotspot. At present, the mould surface hardening methods include coating technologies such as electroplating, plating, thermal spraying, and alloying [1–4], physical modification methods such as high-frequency quenching, flame hardening, and laser heat treatment [5, 6], and chemical treatment methods such as carburizing, nitriding, TD treatment, etc. [7, 8]. Thermal spraying materials are divided into metal powder and ceramic composite powder [9]; the former includes pure metals, alloys, and Ni/Fe/Co/Cu based self-fluxing alloy, and the latter includes metal oxide, metal carbides and borides, silicides and

¹School of Mechanical Engineering, Changzhou University, Changzhou 213164, China. ²Jiangsu Key Laboratory of Materials Surface Science and Technology, Changzhou University, Changzhou 213164, China.

³To whom correspondence should be addressed; e-mail: kong-dejun@163.com.

powder coating, agglomerated powder, etc. The FeCrBSi coating is a Fe-based self-fluxing alloy [10], which is developed on the basis of Fe–Cr–B and FeCrSi coatings, the B element has strong reducibility and the Si compound has good wear resistance, which improve oxidation resistance and wear resistance of the coating.

In China and abroad, the research efforts are concentrated on the microstructures, wear resistance and surface hardness of FeCrBSi coating [11, 12], the bonding mechanism of the FeCrBSi coating and substrate has rarely been reported. In this study, a FeCrBSi coating was prepared on H13 hot work die steel with high-velocity oxygen fuel (HVOF) spraying. The morphologies, plane and line scans, and phases were analyzed with FMS EM, its configured EDS, and XRD, respectively.

The distribution of chemical elements at the coating interface and bonding mechanism were discussed, and the wear performance was also investigated, which provided an experimental basis for HVOF-sprayed FeCrBSi coating on the surface of H13 hot work die steel after modification treatment.

EXPERIMENTAL

The substrate material was H13 hot work die steel, whose hardness was 480 HV after quenching at 1020–1050°C and tempering at 530–560°C for two times. After coarsening with brown corundum sands, the roughness of the substrate measured by using a Mitutoyo surface roughness tester was 0.4 μm. The alloy powder was FeCrBSi with the weight contents of chemical elements as follows (wt.%): 25–28 C, 20–25 Cr, 3–5 B, 3–5 Si, 5–8 Ni, 1–2 W, ≤0.02 S, and Fe being the rest.

The HVOF spraying test was conducted on ZB-2700 high-speed flame spraying equipment by using kerosene as fuel, O₂ as combustion supporting gas, and N₂ as powder feeding gas. Spraying parameters were shown as follows: powder feeding of 110 g/min, spraying gun distance of 250 mm, fuel pressure of 1.25 MPa, oxygen pressure of 1.58 MPa, and spraying gun pressure of 0.95 MPa.

The morphologies and chemical elements of the obtained coating surface and interface were analyzed with JSUPRA55 field emission scanning electron microscopy (FMSEM) and its configured energy spectrometer analysis (EDS), respectively, and the phase compositions were analyzed with a D/max2500PC X-ray diffraction (XRD) tester.

The wear tests were conducted on a CFT-I comprehensive test instrument for surface properties of materials, the sample dimension was 15 mm × 15 mm × 3 mm and diameter of the wear track was 5 mm. The tribopair was Si₃N₄ ball / FeCrBSi coating, the diameter of the Si₃N₄ ball was 5 mm, and the wear test was performed at room temperature, load of 20 N, wear time of 30 min, rotational speed of 500 rpm, and sliding linear speed of 261.7 mm/sec. After the wear test, the morphologies and chemical elements of the worn track were analyzed with JSM-6360LA scanning electron microscopy (SEM) and its configured energy spectrometer analysis (EDS), respectively.

ANALYSIS AND DISCUSSION

Morphologies and XRD Analysis of Powder. Figure 1a shows that the particle sizes of FeCrBSi powder were consistently and uniformly distributed. In Fig. 1b, the FeCrBSi powder was presented with a nearly ball, the skeleton was CrBSi particles, and Fe was the binder. The particle diameter was 50–95 μm, which was not stick with the spraying equipment or other particles, and the dense particles reduced friction effect and increased the particle flow properties in the spraying process. From Fig. 1c, it can be seen that the main phases of the powder were composed of B, CrSi₂, Fe, Fe₂Si, and FeSi, with no other impurities.

Figure 2a shows that the FeCrBSi coating was relatively flat, the roughness of the obtained coating was 0.8 μm, higher by 0.4 μm than that of the substrate, which had a certain effect on wear performance of the coating. The melting effect of sprayed powders was well; there were no obvious convex peaks and pits. Because the powder feeding was relatively large in the spraying process, the powder particles did not turn into a molten state completely, and some part of the powder particles was directly embedded in the sprayed surface with the original particle state. The small holes were unmelted particles falling off from the coating, which had a few effects on the coating performance, as shown in Fig. 2b. The primary phases of the coating were composed of Fe–Cr and Fe phase;

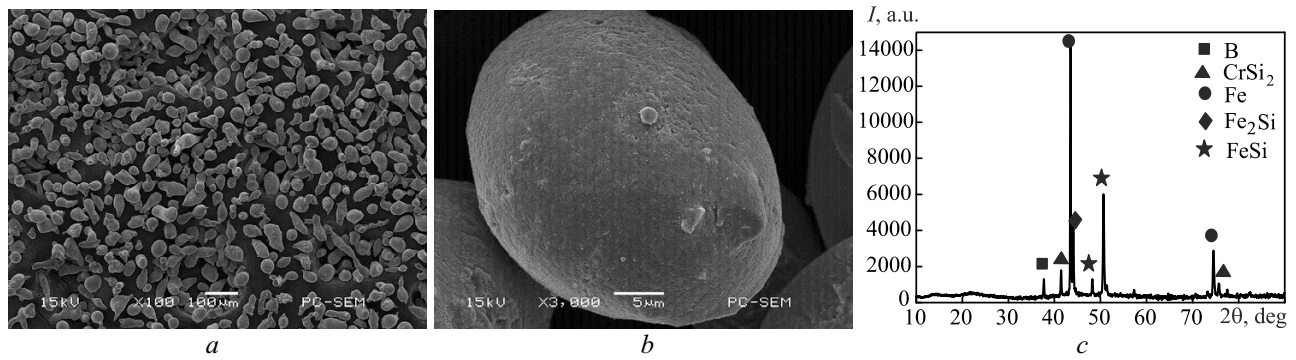


Fig. 1. Morphologies and XRD analysis of FeCrBSi powder: a) low magnification, b) high magnification, and c) XRD analysis

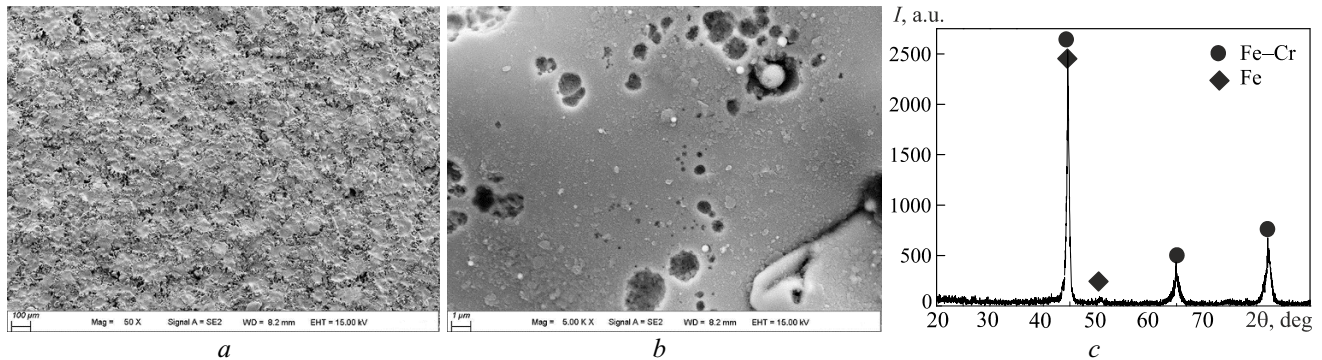


Fig. 2. Surface morphologies and XRD analysis of FeCrBSi coating: a) low magnification, b) high magnification, c) XRD analysis

as shown in Fig. 2c, the B and Si phases were not detected due to the low contents. The hardness of the obtained coating measured by using a HXD-1000TMC type Vickers microhardness tester was 600 HV, which was higher by 120 HV than that of the substrate.

EDS Plane Scan Analysis of Coating Surface. The FeCrBSi coating surface in Fig. 2a was analyzed using a plane scan, the result is shown in Fig. 3a. The weight contents of chemical elements (wt.%) were as follows: 32.57 C, 11.05 O, 0.85 Si, 10.88 Cr, 45.65 Fe; and atomic contents (at.%): 61.57 C, 15.69 O, 0.68 Si, 475 Cr, 17.38 Fe. The Fe, Cr, Si, O and C elements were evenly distributed, as shown in Fig. 3b–f. There was no atom-rich and atom-poor regions, which was conducive to improving the integrity and wear performance of the coating. The Cr and C contents in the coating were high, resulting in a large number of carbides such as Cr_{23}C_6 and Cr_7C_3 ; among them, the microhardness of Cr_7C_3 reached 1450 HV, which was the primary hard phase of the coating. The coating structure was Fe–Cr solid solution, dispersing the hard phases of Cr_{23}C_6 and Cr_7C_3 with good thermal stability, which protected the substrate from oxidizing.

EDS Plane Scan Analysis of Coating Interface. Figure 4a shows the plane scanned position of the coating interface, the coating microstructure was uniform and was bonded closely with the substrate, no obvious cracks. Only a small number of porosities existed, and the layered structure of the coating was not very obvious. The result of plane scan analysis is shown in Fig. 4b; the weight contents of chemical elements were as follows (wt.%): 28.83 C, 6.05 O, 0.28 Al, 0.87 Si, 0.28 S, 0.42 V, 674 Cr, 54.97 Fe, 1.57 W; and atomic contents (at.%): 60.67 C, 955 O, 0.26 Al, 0.79 Si, 0.22 S, 0.21 V, 3.27 Cr, 24.86 Fe, 0.22 W. The peak of Fe element was the highest, and that of C, Cr, B, and Si elements was high, which indicated that the coating interface was primarily composed of Fe, C, Cr, B, and Si elements. The Fe element was uniformly distributed at the interface, which was the same content at different depths, as shown in Fig. 4c. The divided line was not obvious between the coating and the substrate, indicating that the mechanical bonding was good at the interface. The Cr content in the coating was high, as shown

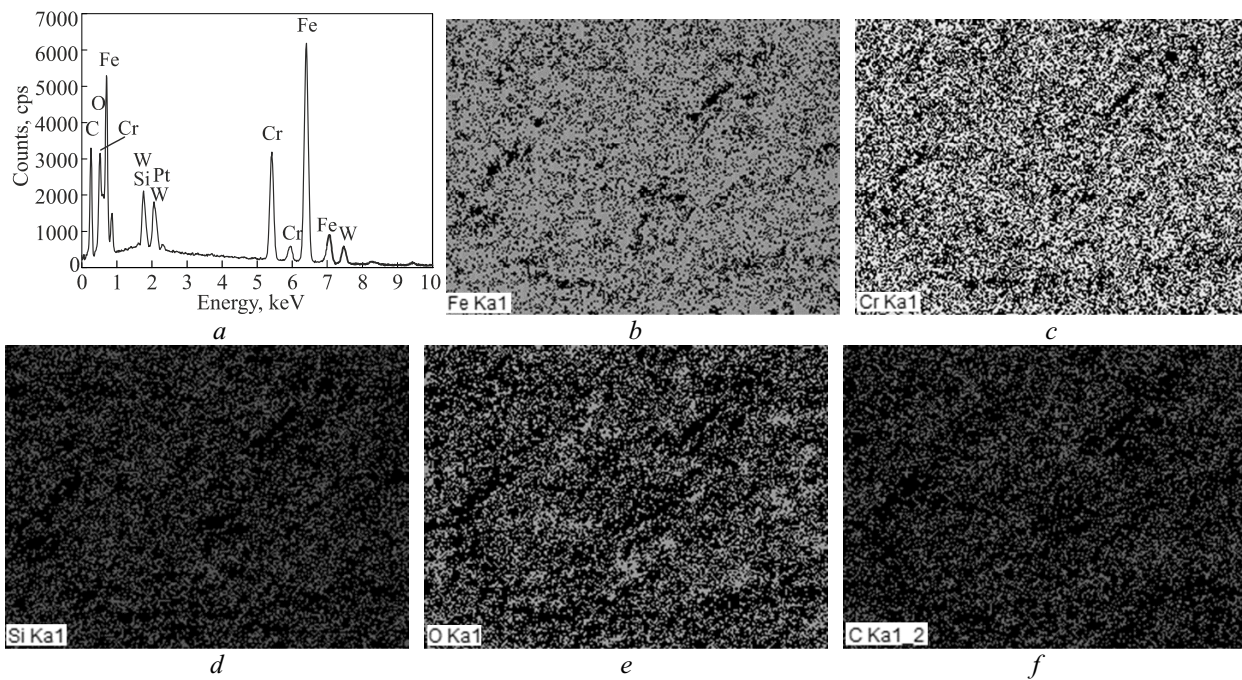


Fig. 3. Plane scan analysis of FeCrBSi coating surface: a) result of plane scans, b) Fe content, c) Cr, d) Si, e) O, and f) C content

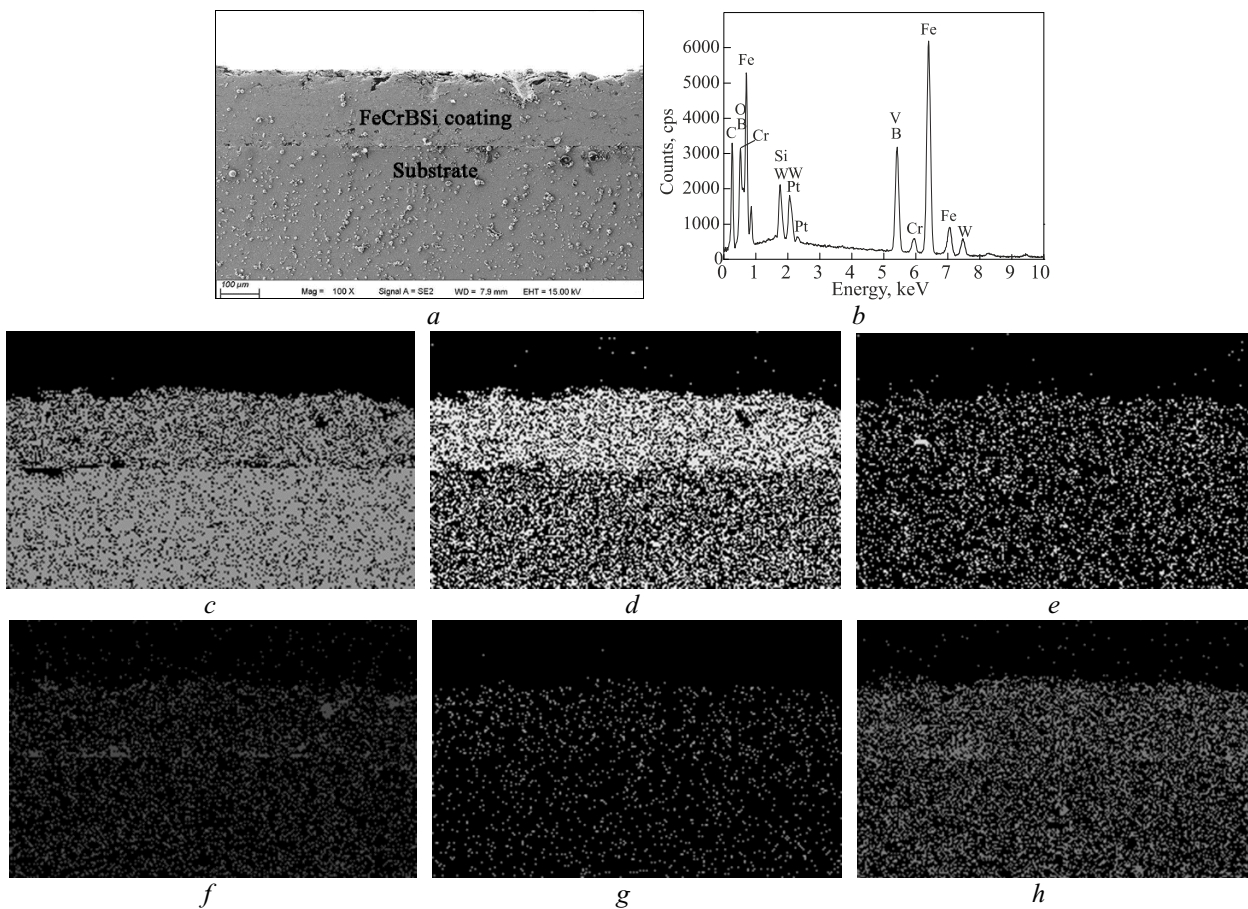


Fig. 4. Plane scan analysis of FeCrBSi coating interface: a) interface morphology, b) result of plane scans, c) Fe content, d) Cr, e) B, f) Si, g) O, and h) C content

in Fig. 4d, playing a role of binder in the thermal spraying process. Figure 4e shows the distribution of B elements: B was also uniformly distributed at different depths, and the coating and the substrate at the interface had a certain content of B. Figure 4f shows the distribution of Si element; during oxidation of the substrate surface, the Si element appeared in the atom-rich region on the substrate surface and generated Fe_2SiO_4 with Fe of the substrate, embedding in grain boundaries of the substrate surface, which improved bonding strength of the coating and the substrate. Figure 4g shows the distribution of O element at the interface; there was no atom-rich phenomenon, showing that the oxidized elements were fewer in the spraying process, and the effects on the interface were small. Figure 4h shows the distribution of C element, the coating and the substrate had a certain content of C.

EDS Line Scan Analysis of Coating Interface. Figure 5a shows the line scanned position of the FeCrBSi coating interface. As seen from Fig. 5b, the Fe element showed a decreasing trend in the direction from the substrate to the coating and the Fe element in the substrate did not diffuse into the coating. Figure 5c shows the line scan distribution of Cr element at the interface; the Cr content in the coating was high, and produced the diffusion into the substrate. Figure 5d shows the line scan distribution of B element at the interface; the B content in the coating was high, and that in the substrate was low, there was no diffusion phenomenon. Figure 5e shows the line scan distribution of Si element at the interface; the Si content gradually reduced in the direction from the coating to the substrate. Figure 5f shows the line scan distribution of O element at the interface, the O content in the coating was almost the same as that in the substrate. Figure 5g shows the line scan distribution of C element at the interface; the O element almost existed in the substrate, no C in the coating.

The Cr content at the interface was high; this was because a part of FeCrBSi reacted with O_2 to form oxides in the spraying process, the O content at the interface was significantly higher than that of the coating and the

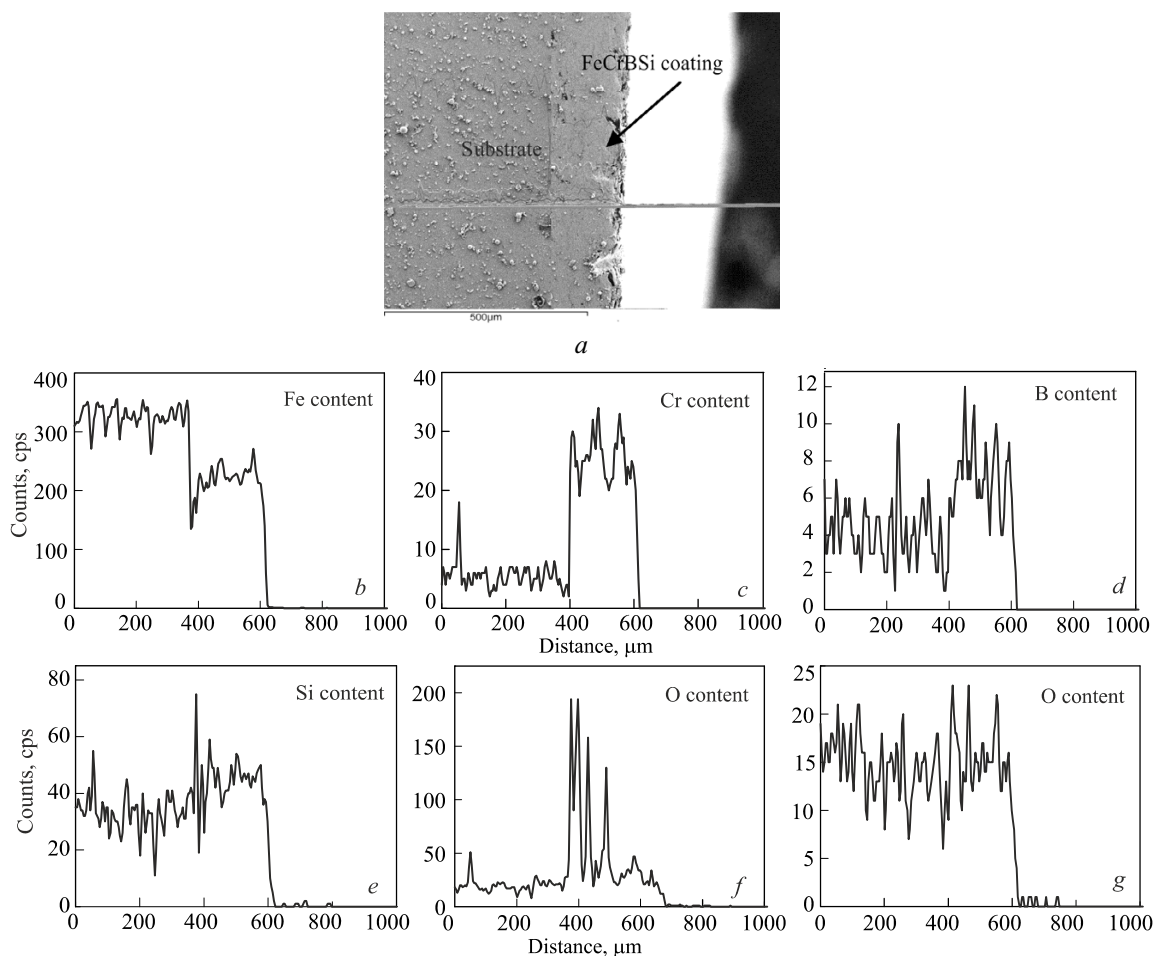


Fig. 5. Line scan analysis of FeCrBSi coating interface: a) interface morphology, b–g) elements content

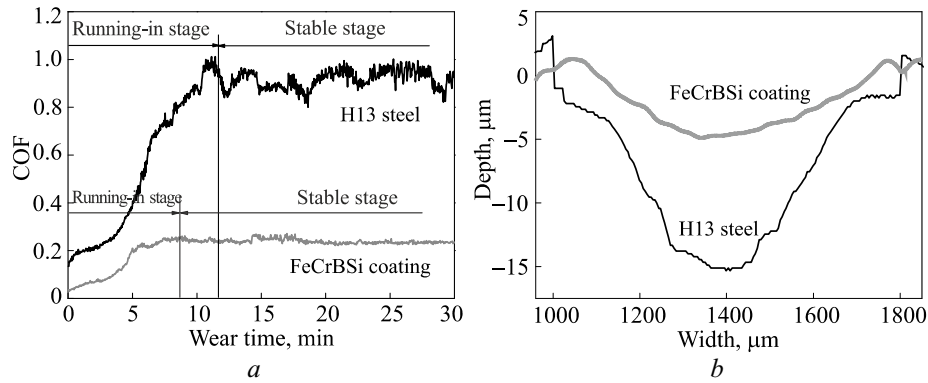


Fig. 6. COFs vs wear time and wear profile: a) COFs vs wear time, b) wear profile

substrate. The Cr, Si, and B contents decreased slowly from the coating to the substrate, the descent gradient at the interface was relatively small and no mutant, indicating that there was thermal chemical reaction and element penetration phenomenon at the interface, and Cr, Si and B of the coating appeared to obviously diffuse to the substrate. The Fe content slowly increased from the coating to the substrate, and slow transition occurred at the interface, which indicated that Fe of the substrate had certain diffusion to the coating. From the curves of line scan analysis, the Fe, Si, and B elements had gradually decreased, indicating that these elements diffused into the substrate, which had homogenizing effect on the coating microstructures and improved the bonding state at the interface by forming metallurgical bonding.

COFs and Wear Profile. The average COF of H13 steel was 0.7692, while that of the coating was only 0.2126, decreased by 72%, as shown in Fig. 6a, which indicated that the FeCrBSi coating had good friction resistance. The wear process of the coating was divided into running-in period and normal wear period.

During the running-in period (0–8 min), the COFs of the coating were small, and the average COF was 0.1391. This was because the contact surface between the micro convex body and the wear debris gradually increased with increasing wear time; therefore, the COFs were also shown as an increasing phenomenon. With

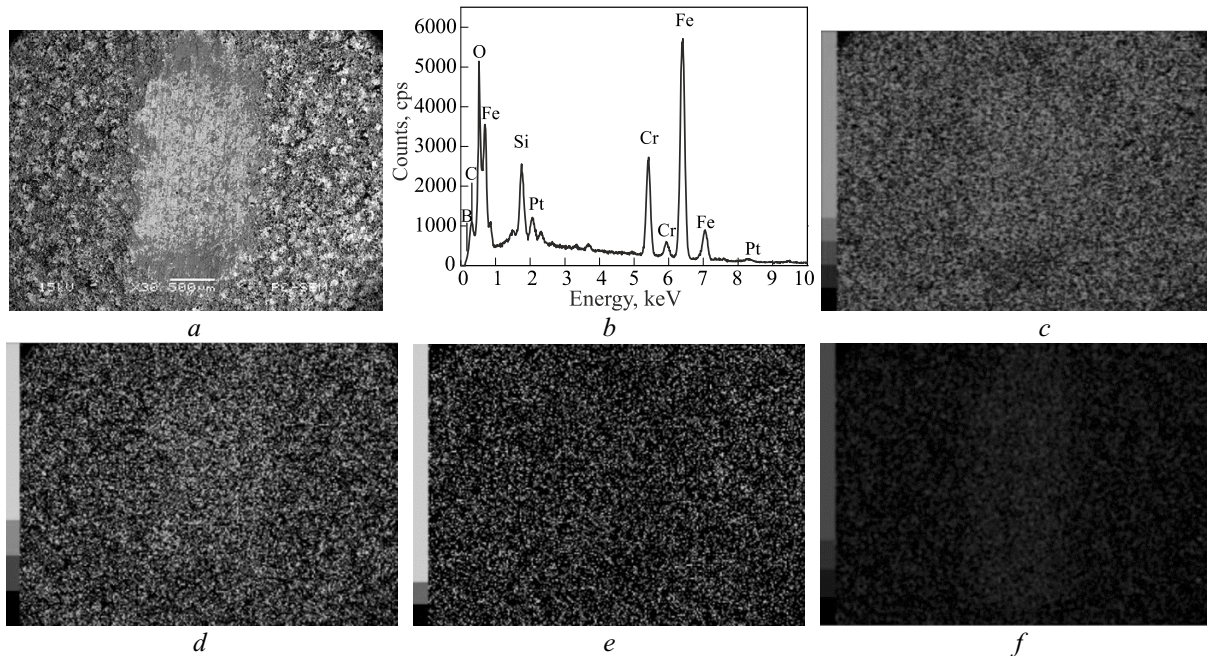


Fig. 7. Plane scan analysis of worn track on FeCrBSi coating: a) position of plane scan analysis, b) result of plane scan analysis, c) Fe content, d) Cr content, e) B content, f) Si content

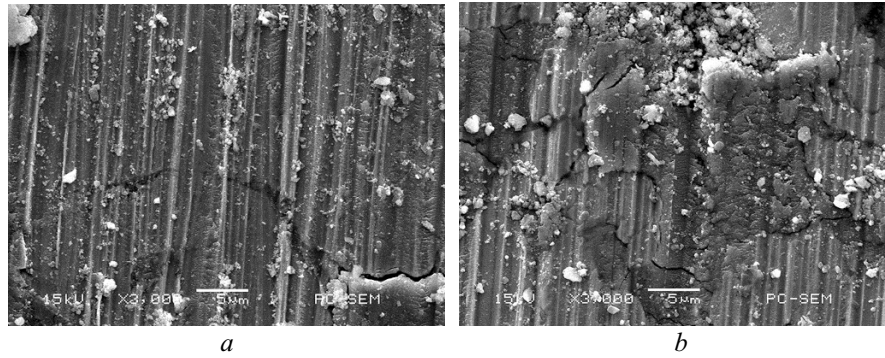


Fig. 8. Worn morphologies of FeCrBSi coating: a) abrasive wear, b) spalling

friction continuing, the worn particles migrated to maintain a balance, the friction tended to be stable [13]. After entering normal wear period (8–30 min), the average COF was 0.2394, and the value was small. The wear depth of H13 steel was 15.33 μm , while that of the coating was only 4.89 μm , decreased by 68.1%, as shown in Fig. 6b. The wear rate of H13 steel and coating was $4.7 \cdot 10^{-6} \text{ mm}^3/\text{sec} \cdot \text{N}$ and $1.5 \cdot 10^{-6} \text{ mm}^3/\text{sec} \cdot \text{N}$, respectively, indicating that the wear resistance of FeCrBSi coating was significant.

Worn Morphologies. The plane scanned position of the coating is shown in Fig. 7a, the surface of worn track was relatively flat. The weight contents of chemical elements were shown as follows (wt.%): 74.30 Fe, 16.33 Cr, 0.44 B, 1.88 Si, 0.67 C, 6.39 O; and atomic contents were shown as follows (at.%): 60.90 Fe, 14.45 Cr, 0.64 B, 3.08 Si, 2.55 C, 18.39 O. The Fe, Cr, and B elements on the worn track were uniformly distributed and did not produce the atoms-poor region, as shown in Fig. 7c–e. Compared with the element distribution on the coating surface, the element distribution in the worn track did not change significantly, which indicated that the friction process was stable and consistent with the test results of COFs in Fig. 6a. The Si element on the worn track produced the atom-rich region, as shown in Fig. 7f, which was due to the sticking of Si elements from ceramic balls on the worn track.

The wear of the coating was more serious; there was obviously a wide and deep worn track, presenting the mechanism of abrasive wear, as shown in Fig. 8a. At the same time, the coating surface appeared to have serious cracks and peeling phenomenon, as shown in Fig. 8b. This main source was shown as follows [14, 15]: i) the boride hard phase fell off from the coating under the action of frictional load; ii) the residual stresses produced microcracks, resulting in brittle falling off during HVOF spraying; iii) the oxide film generated in the process of wear appeared to show brittle spalling.

Therefore, the wear mechanism of the coating primarily consisted in abrasive wear and spalling.

CONCLUSIONS

The FeCrBSi particles are completely melted by HVOF process, the melted powders produce deformation after contacting the substrate with better dispersion, and the coating is composed of Fe–Cr and Fe phases. The Cr, Si, and B elements are enriched in the coating at the interface, forming the alloy layer, which improves the wear performance of the substrate.

The Fe, Si, and B elements in the coating diffused into the substrate and the interface achieves a certain metallurgical combination, which is conducive to improve bonding strength of the coating interface.

The HVOF-sprayed FeCrBSi coating has excellent friction performance, the average COF is 0.2126, and the wear mechanism primarily consists in abrasive wear and spalling.

ACKNOWLEDGMENTS

Financial support for this research by the Jiangsu Province Science and Technology Support Program (Industry) (BE2014818) is gratefully acknowledged.

REFERENCES

1. M. J. Arab, M. Farzam, and H. Zohdirad, "Wear and corrosion resistance and electroplating characteristics of electrodeposited Cr–SiC nano-composite coatings," *Trans. Nonferrous Met. Soc. China*, **23**, No. 7, 1993–2001 (2013).
2. P. L. Ge, M. D. Bao, H. J. Zhang, et al., "Effect of plasma nitriding on adhesion strength of CrTiAlN coatings on H13 steels by closed field unbalanced magnetron sputter ion plating," *Surf. Coat. Technol.*, **229**, No. 9, 146–150 (2013).
3. J. G. Gregory and G. H. Robert, "Thermal-sprayed coatings on aluminum for mould tool protection and upgrade," *J. Mater. Process. Technol.*, **204**, No. 1–3, 184–191 (2008).
4. K. Y. Lee, S. Choi, J. Suh, and C. Y. Kang, "Effect of laser power and powder feeding on the microstructure of laser surface alloying hardened H13 steel using SKH51 powder," *Mater. Des.*, **95**, No. 1, 173–182 (2016).
5. J. Wang, J. F. Gu, X. X. Shan, et al., "Numerical simulation of high pressure gas quenching of H13 steel," *J. Mater. Process. Technol.*, **202**, No. 1–3, 188–194 (2008).
6. I. A. Figueroa, I. Betancourt, G. Lara, and J. A. Verduzco, "Effect of B, Si, and Cr on the mechanical properties of Fe-based amorphous metallic ribbons," *J. Non-Cryst. Solids*, **351**, No. 37–39, 3075–3080 (2005).
7. G. Castro, A. Fernández-Vicente, and J. Cid, "Influence of the nitriding time in the wear behavior of an AISI H13 steel during a crankshaft forging process," *Wear*, **263**, No. 7–12, 1375–1385 (2007).
8. C. Zhang, L. Liu, K. C. Chan, et al., "Wear behavior of HVOF-sprayed Fe-based amorphous coatings," *Intermetallics*, **29**, No. 29, 80–85 (2012).
9. W. H. Liu, F. S. Shieu, and W. T. Hsiao, "Enhancement of wear and corrosion resistance of iron-based hard coatings deposited by high-velocity oxygen fuel (HVOF) thermal spraying," *Surf. Coat. Technol.*, **249**, No. 7, 24–41 (2104).
10. L. N. Zhu, B. S. Xu, H. D. Wang, and C. B. Wang, "Determination of hardness of plasma-sprayed FeCrBSi coating on steel substrate by nanoindentation," *Mater. Sci. Eng. A*, **528**, No. 1, 425–428 (2010).
11. L. N. Zhu, B. S. Xu, H. D. Wang, and C. B. Wang, "On the evaluation of residual stress and mechanical properties of FeCrBSi coatings by nanoindentation," *Mater. Sci. Eng. A*, **536**, No. 3, 98–102 (2012).
12. R. Gonzalez, M. A. Garcia, I. Penuelas, et al., "Microstructural study of NiCrBSi coatings obtained by different processes," *Wear*, **263**, No. 1–6, 619–624 (2007).
13. X. H. Wang, M. Zhang, X. M. Liu, et al., "Microstructure and wear properties of TiC/FeCrBSi surface composite coating prepared by laser cladding," *Surf. Coat. Technol.*, **202**, No. 15, 3600–3606 (2008).
14. Y. B. Wang, S. S. Zhao, W. Y. Gao, et al., "Microstructure and properties of laser cladding FeCrBSi composite powder coatings with higher Cr content," *J. Mater. Process. Technol.*, **214**, No. 4, 899–905 (2014).
15. Y. H. Qing, "Influence of molybdenum on the microstructure and properties of a FeCrBSi alloy coating deposited by plasma transferred arc hardfacing," *Surf. Coat. Technol.*, **225**, No. 25, 11–20 (2013).